Journal of Materials Processing Technology 237 (2016) 88–95

Contents lists available at ScienceDirect

Journal of Materials Processing Technology

journal homepage: www.elsevier.com/locate/jmatprotec

Design of a gas forming technology using the material constants obtained by tensile and free bulging testing

Sergey A. Aksenov[a,*], Aleksey V. Kolesnikov[b], Anastasia V. Mikhaylovskaya[c]

[a] National Research University Higher School of Economics, Department of Applied Mathematics, 123458 Tallinskaya 34, Moscow, Russia
[b] National Research Irkutsk State Technical University, Laboratory of Progressive Forming Methods in Harvesting and Stamping Production, 664074, Lermontova 83, Irkutsk, Russia
[c] National University of Science and Technology "MISiS", 119049, Leninsky Prospekt, 4, Moscow, Russia

ARTICLE INFO

Article history:
Received 25 November 2015
Received in revised form 2 May 2016
Accepted 4 June 2016
Available online 5 June 2016

Keywords:
Material characterization
Biaxial tension
Free bulging
Tensile test
Superplastic forming
Finite element simulation

ABSTRACT

Uniaxial tensile testing is a most common way of obtaining the information about the constitutive behavior of a material during gas forming. At the same time for industrial applications it is important to know the material behavior in a biaxial tension mode, which is much closer to the one realized in a shell during forming process. The paper focused on the investigation of the differences between the gas forming technologies designed in FEM based CAE system using the material parameters obtained in conditions of uniaxial and biaxial tension. The rheological characteristics of AMg6 aluminum alloy obtained by tensile and free bulging testing are analyzed and compared. The comparison shows that the constitutive data obtained by these methods are different. The effect which these differences could provide to the design of a gas forming technology was studied. A pressure regime for an aircraft part forming which maintains the maximum strain rate at constant level was calculated using finite element simulation for the both sets of constitutive constants. The calculated pressure regimes were then realized experimentally and the differences between the deformed specimens were analyzed.

1. Introduction

Gas forming technology is a method of production of thin sheet parts used mainly in aerospace industry. A sheet specimen is climbed between a dies and formed by pressure of inert gas. Automated pressure controlling systems make it possible to realize superplastic or quasi-superplastic forming regimes ensuring better plasticity of a material. Such technological processes are designed using computer simulations realized in modern finite element method (FEM) based systems.

The accurate describing of constitutive behavior of a material is a key point to the design of forming technologies. Tensile testing is a most common way providing the information about constitutive behavior of a material. At the same time, the data obtained by this way are usually not accurate enough for construction of realistic models of gas forming processes. One of the possible reasons is that during the gas forming the biaxial tension stress mode predominates in the material volume since the stress mode in tensile testing is uniaxial tension. The way of cavitation and microstructure development is different in these different stress modes what can cause the differences in constitutive behavior. Moreover, irregular thinning and necking accruing in tensile tests may produce additional errors. Nazzal et al. (2011) investigated the effect of specimen geometry in superplastic tensile tests. They found that variations in specimen geometry could lead to large disparities in testing results.

In order to avoid the complications, listed above, the corrections of constitutive data obtained by tensile tests are required. These corrections can be provided by additional free bulging testing which produce the biaxial tensile stress mode in the material. Such an approach was used by Albakri et al. (2013) for correction of tensile test data previously obtained by Abu-Farha and Khraisheh (2007) for AZ31 magnesium alloy. Other way, is the determination of constitutive constants by the free bulging tests directly.

Since free bulging tests do not provide the stress-strain rate data directly, different methods were developed to interpret their results. Most of them provide the way to get the constants of a power law constitutive model:

$$\sigma_e = K\dot{\varepsilon}_e^m \varepsilon_e^n \quad (1)$$

Where σ_e is effective stress; $\dot{\varepsilon}_e$ is effective strain rate; ε_e is effective strain; K, m and n are the characteristics of the material. If the strain hardening is neglected ($n = 0$), the Eq. (1) is similar to

* Corresponding author.
E-mail addresses: saksenov@hse.ru, aksenov.s.a@gmail.com (S.A. Aksenov).

http://dx.doi.org/10.1016/j.jmatprotec.2016.06.003
0924-0136/

the one proposed by Backofen et al. (1964) for describing of superplastic materials flow behavior. This power law equation do not contain any information about the microstructure development and different deformation mechanisms taking place during superplastic deformation which can be taken into account by complex physically-based constitutive models as the ones recently investigated by Alabort et al. (2015). At the same time the Eq. (1) can be adopted as a simple approximation of material properties in a limited strain-rete range and used for the computer simulation of modern SPF technologies. Zhao et al. (2010) used this equation to describe the material properties for three dimensional finite element simulation of a hollow blade forming process. Luckey Jr. et al. (2009) developed a two-stage SPF technology to improve the thickness profile of the final part. As a constitutive equation they used the Eq. (1) with the material constants determined by Raman et al. (2007).

The geometrical data of the domes obtained by free bulging of circular diaphragm under constant pressure can be used to evaluate the constants of Eq. (1). Enikeev and Kruglov (1995) introduced a method for evaluation of the material constants using free bulging tests carried out to a predetermined dome height. El-Morsy et al. (2001) introduced the characterization technique based on a multi-dome forming test. Giuliano and Franchitti (2007) proposed a method for characterization of superplastic materials which is able to evaluate a strain hardening index n as well as the constants K and m. Li et al. (2004) simulated bulging processes by finite element method (FEM) and applied an inverse analysis to obtain the constants K and m neglecting strain hardening index n. Recently Sorgente and Tricarico (2014) used inverse analysis based on FEM for characterization of the superplastic aluminum alloy ALNOVI-U. Aksenov et al. (2015) proposed a characterization technique based on inverse analysis and semi-analytical model describing the evolution of dome height during the test.

The particular objective of this work is to investigate the differences of the gas forming technologies designed in a FEM based CAE system using material parameters obtained by different ways. In the design of superplastic forming (SPF) technologies the pressure regimes are calculated to maintain the strain rate value on a certain constant level. The material constitutive constants are the important inputs of such calculations. Thus the question of how the accuracy of these input data affects the designed technological regimes deserves proper attention.

The forming process of a special industrial shell detail was considered. The material (AMg6 aluminum alloy in as received condition) and the process temperature (415 °C) were taken as initial technological restrictions. Two sets of material constants describing its behavior at 415 °C were obtained separately using free bulging tests and tensile tests. These constants were then used for simulation of forming process. Gas pressure regimes were calculated to provide the maximum strain rate at the same constant value for the both cases. The obtained pressure regimes were then realized till the predicted moments of the first contact between the specimen and the die and the results were compared with the prognosis made by computer simulation.

2. Evaluation of constitutive constants

2.1. Material

The AMg6 alloy (Mg-6%, Mn-0.65%) is used in the investigated process. This is an aluminum based alloy of the Al-Mg-Mn system which is used in many industries including aerospace and civil engineering. Superplastic behavior of the AMg6 alloy was studied by Valiev and Kaibyshev (1983). It was shown that after proper grain preparation procedures the alloy can demonstrate superplastic behavior. Kaibyshev (1984) obtained the constitutive constants for this alloy at the temperature of 420 °C and initial average grain size of 9.5 μm. He found that at the given conditions the m value is about 0.45 and the alloy can be deformed at to 410% elongation at the strain rate of 0.6×10^{-3}. Similar Al-Mg alloy was studied by Guo et al. (1990) in temperature range from 470 to 530 °C. They found that the material can display a superplastic effect at these temperatures having the best plasticity at 490 °C. Chuvil'deev et al. (2008) investigated the improvement of the mechanical properties of the AMg6 alloy, which can be achieved by equal cheval pressing. Portnoy et al. (2013) analyzed the superplastic behavior the AMg6 alloy and effect of chromium addition on grain refinement and superplasticity. Recently the deformation and recrystallization textures of AMg6 alloy after hot extrusion were studied by Rusakov et al. (2015).

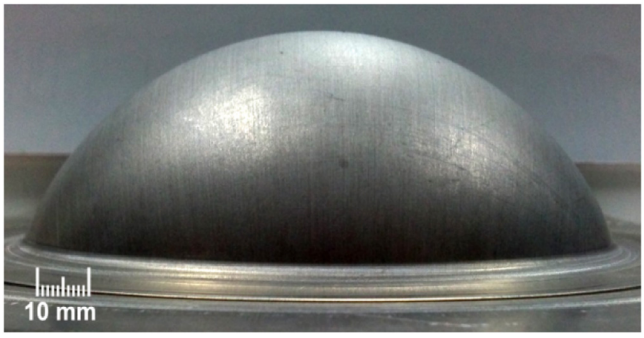

Fig. 1. Specimen formed at the pressure of $P_3 = 0.3$ MPa during 3500 s.

In many industrial cases it is possible to avoid the microstructure preparation requiring complicated processing steps and use the material in as received condition. This possibility is discussed by Woo et al. (1997). They investigated Al-Mg alloys containing 5.3, 7 and 11 wt.% of Mg in the temperature range of 300–550 °C and strain rate range $0.5*10^{-4}$ to 10^{-1}. Steady state stress—strain rate curves are presented and it is noted than they can be fitted by Backofen equation with the m value equal to 0.3 for each temperature and chemical composition if the strain rate is less than 10^{-2}. The elongations reached at the temperature of 400 °C and the strain rates of 10^{-3} and 10^{-2} are in the range of 200–275%. Lower temperatures and higher strain rates leads to abrupt decreasing of tensile ductility.

Due to the initial industrial restrictions, the forming temperature was chosen at 415 °C. Two series of tensile and free bulging tests were performed at this temperature on hot rolled sheets of a 0.92 mm mean initial thickness. In both cases the specimens were annealed during 20 min before the deformation and then deformed in argon atmosphere. Microstructure analysis showed that average grain size was 9.5 ± 0.7 μm before and 10.5 ± 0.7 μm after the annealing.

2.2. Free bulging testing

The experimental conditions of free bulging tests used in this study and the characterization technique used for their interpretation were described by the authors previously (Aksenov et al., 2015). The tests were performed at five different pressures: $P_1 = 0.3$, $P_2 = 0.35$, $P_3 = 0.4$, $P_4 = 0.5$ and $P_5 = 0.6$ MPa; with different forming times t_i. The specimens were formed to a cylindrical die of a 50 mm diameter and 5 mm entry radius. Each specimens was measured after the forming to obtain the values of the dome height (H_i^{exp}) and thickness at the apex (s_i^{exp}). A photograph of the specimen formed at the pressure of 0.3 MPa during 3500 s showed in Fig 1. The results of the tests are presented in Table 1 which is also contains the values of mean strain rate calculated as final strain divided on forming

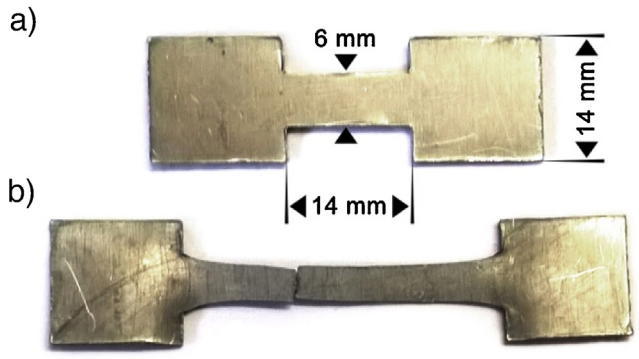

Fig. 2. Specimen before (a) and after (b) deformation with constant strain rate of $10^{-4}\,s^{-1}$.

Table 1
The results of free bulging tests.

P,MPa	t, s	H,mm	s/s0,–	Mean strain rate,$10^{-3}s^{-1}$
0.3	500	20.95	0.823	0.391
0.3	750	22.25	0.785	0.323
0.3	1000	24.5	0.746	0.293
0.3	1500	27.85	0.704	0.234
0.3	2000	29.3	0.668	0.201
0.3	2500	31.95	0.597	0.207
0.3	3000	35.5	0.543	0.204
0.3	3500	37.35	0.483	0.208
0.3	4000	44.05	0.409	0.224
0.3	4244	47.8	0.395	0.219
0.35	1000	28.3	0.679	0.387
0.35	1500	33.4	0.613	0.326
0.35	2000	41.7	0.462	0.386
0.35	2515	47.35	0.291	0.491
0.4	500	26	0.726	0.642
0.4	1000	35.4	0.551	0.596
0.4	1250	40.5	0.463	0.616
0.4	1534	47.7	0.287	0.813
0.5	180	24.5	0.735	1.707
0.5	360	31	0.632	1.276
0.5	540	38.4	0.485	1.341
0.5	576	44.2	0.381	1.675
0.6	90	24.15	0.737	3.393
0.6	180	30.65	0.620	2.656
0.6	270	38.6	0.466	2.826
0.6	305	45.3	0.383	3.147

time. The strain rates are in the range of 2.0×10^{-4}–3.0×10^{-3} and grow with the pressure.

The geometrical data (H_i^{exp} and s_i^{exp}) obtained experimentally were processed by inverse analysis in order to determine the material constants m and K. The target function was constructed as a cumulative quadratic deviation between the measured and predicted values of a dome height and thickness:

$$F=\sum_{i=1}^{N}\left\{\left(\frac{H_i^{exp}-H(t_i)}{H_i^{exp}}\right)^2+\left(\frac{s_i^{exp}-s(t_i)}{s_i^{exp}}\right)^2\right\} \quad (2)$$

where N = 26 is a total number of the experiments, $s(t)$ and $H(t)$ are the predicted evolutions of a dome height found as the solutions of following differential equations:

$$\frac{dH}{dt}=\frac{\rho}{A}\left(\frac{P\rho}{2K}\right)^{\frac{1}{m}}s^{1-\alpha-\frac{1}{m}} \quad (3)$$

$$\frac{\partial s}{\partial H}=-\frac{As^{\alpha}}{\rho} \quad (4)$$

where P is applied pressure, ρ—is the dome radius at intense t, A and α are the constants determined by approximation of the experimental $H-s$ data for each particular pressure.

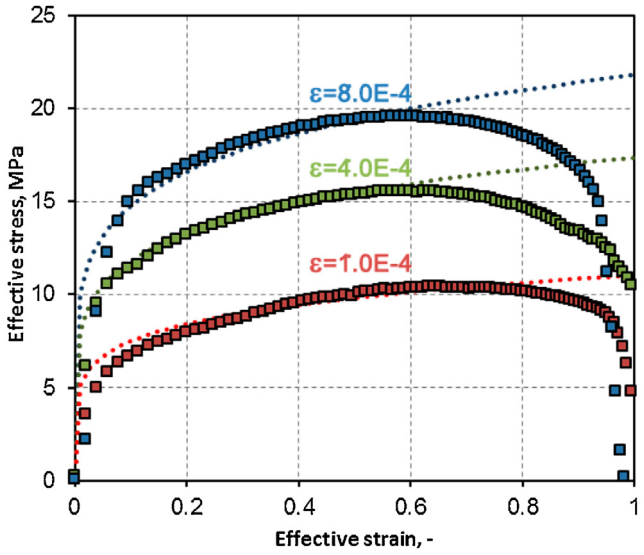

Fig. 3. Stress-strain curves obtained by the constant strain rate tensile tests (markers) and approximation constructed using Eq. (1) (dotted lines).

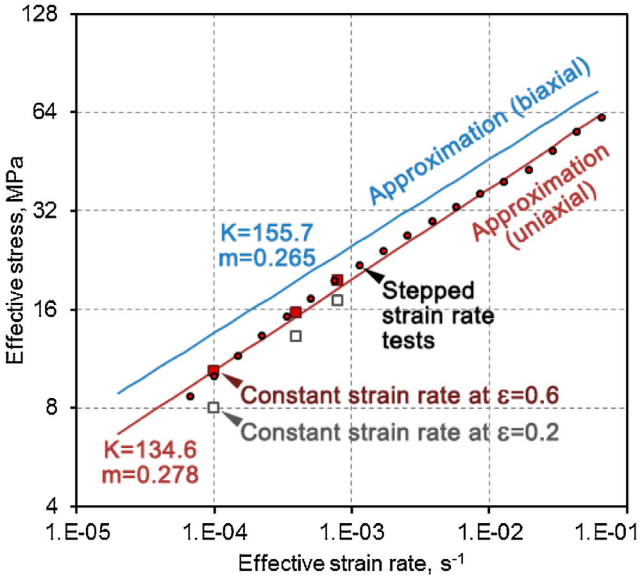

Fig. 4. Results of tensile tests and constitutive equations obtained in uniaxial and biaxial conditions plotted in logarithmic scale.

As a result the Backofen constitutive constants were found as: $K=155.7$ and $m=0.265$. The characterization technique described above was later modified by the authors in order to obtain the constitutive constants of Eq. (1) taking into account the strain hardening index n (Aksenov et al., 2016). It was shown that the strain hardening value obtained by inverse analysis is negligible for the investigated alloy.

2.3. Tensile testing

Tensile tests were performed on the samples machined from as received AMg6 sheets to initial geometry, shown in Fig. 1(a). Two series of tests were performed to characterize the material in conditions of hot forming at the temperature of 415 °C: constant strain rate tests (Fig. 3) and stepped strain rate tests (Fig. 4). The stepped strain rate tests were performed with the strain rate changing in the range of 0.5×10^{-1}–$0.5\times10^{-5}\,s^{-1}$ covering the strain

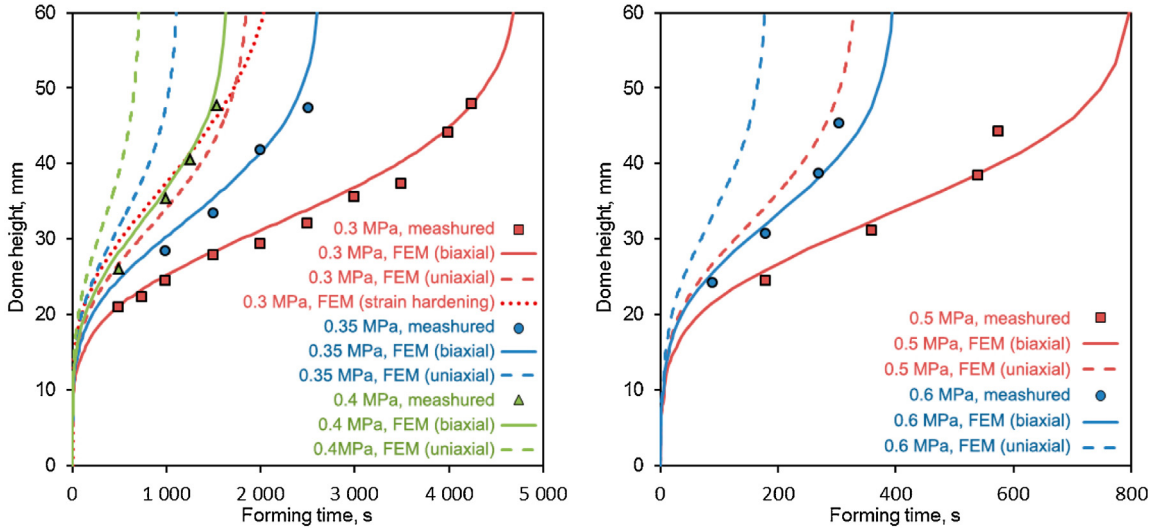

Fig. 5. The evolutions of the dome height predicted by FEM using the material constants obtained by tensile (dashed and dotted lines) and free bulging (solid lines) tests compared with the experimental data (markers).

rates estimated for free bulging tests. The results were approximated by Backofen power law and the rheological constants of the material were found as: $K = 134.6$ and $m = 0.278$. The strain rate of 10^{-3} s^{-1} was chosen as maximum strain rate for the design of forming technology as the corresponding effective stress value ensures relatively low load on the forming equipment.

In order to verify these values and study the effect of strain on the material behavior, three tensile tests were performed at the constant strain rates: 1.0×10^{-4}, 4.0×10^{-4} and 8.0×10^{-4} s^{-1}. The strain rate values were chosen to cover the range of 10^{-4}–10^{-3} s^{-1} which is lower than maximum strain rate considered at 10^{-3} and intersects with the strain rate range realized in free bulging tests. The appearance of specimen deformed at 4.0×10^{-4} s^{-1} is presented at Fig. 2. The stress-strain curves obtained by constant strain rate tests are presented in Fig. 3. Strain hardening can be observed at the beginning of deformation when the effective strain (ε_e) is less than 0.4. In the strain range of 0.4–0.8 the stress-strain curves are almost horizontal and the maximum of each curve corresponds to $\varepsilon_e = 0.6 \pm 0.03$. When the strain is higher than 0.8 the stress is decreasing till the failure at the strain value corresponding to 170% elongation. Rising part of the stress strain curves can be approximated by the Eq. (1) and the material constants can be found at $K = 223.7$, $m = 0.327$ and $n = 0.169$. Due to nonzero value of n the K value is higher in the second model. The value of m is of the same order that the Backofen one. The approximation is shown at Fig. 3 by the dotted lines.

Fig. 4 illustrates the comparison between the results of stepped strain rate tests, constant strain rate tests and the approximations constructed for the biaxial and uniaxial cases plotted in logarithmic scale. Comparing the values of rheological constants and the approximations obtained for the biaxial and uniaxial tension modes it can be noticed that tensile tests produce lower stress data than the ones produced by free bulging tests. Power law constitutive equations plotted in logarithmic scale appear as straight lines with a similar slope which means that the m values, obtained in different stress modes, are very close.

The maximum effective stress values obtained by tensile testing at constant strain rates agree with the ones obtained by the tests with stepped strain rate variation. At the same time the stress values at the strain of 0.2 are lower than the ones obtained at stepped strain rate tests thus the Backofen approximation constructed by stepped tests generally overestimates tensile stress values obtained at constant strain rates. The approximation constructed using Eq. (1) is in very good agreement with the constant strain rate tensile data until the strain is less than 0.6. At the higher strains this approximation deviates from measured values significantly.

The m values of Backofen equation are a bit lower than 0.3 and very close to each other (0.265 and 0.278). Thus, the flow type for this alloy could be treated as quasi-superplastic. These results agree with the ones found by Woo et al. (1997) for the similar alloys and temperatures. Such values of m are typical for the AMg6 alloy in as received condition.

3. Finite element simulation

3.1. FE simulation of a free bulging process

Commercial FEM based CAE system MSC.MARC was used to simulate a free bulging process in order to validate the constitutive constants obtained in a previous section. Five simulations with different pressure values were performed for each pair of Backofen constitutive constants. In addition some simulations were performed using the Eq. (1) constructed on a base of constant strain rate tensile tests and taking strain hardening effect into account. The die geometry described in Section 2.2 and four-node shell elements for specimen discretization were used in the simulations. The dome height evolutions obtained by simulations are presented in Fig. 5.

It can be seen from Fig. 5 that the results of simulations performed for each pressure using different constitutive models do not agree with each other. The results corresponding to the constitutive characteristics obtained in biaxial stress conditions correlates with the experimental data. Using the constitutive constants obtained by tensile tests, results to a very fast growth of a predicted dome height. The time needed to form a dome of a particular height according to these predictions is about a half of the one taken from experimental data. The results of simulation performed using the constitutive model with nonzero strain hardening index at the pressure of 0.3 MPa is illustrated by dotted line.

As the stress values obtained for uniaxial tension mode are lower than the ones obtained in biaxial mode the predicted dome height grows faster for the same pressure. Dew to the same reason the dotted line in Fig. 5 passes above the dashed line till the dome height is lower when 50 mm (which is equal to the die radius) because the stress values produced by corresponding constitutive model are lower than the ones obtained by Backofen equation. The

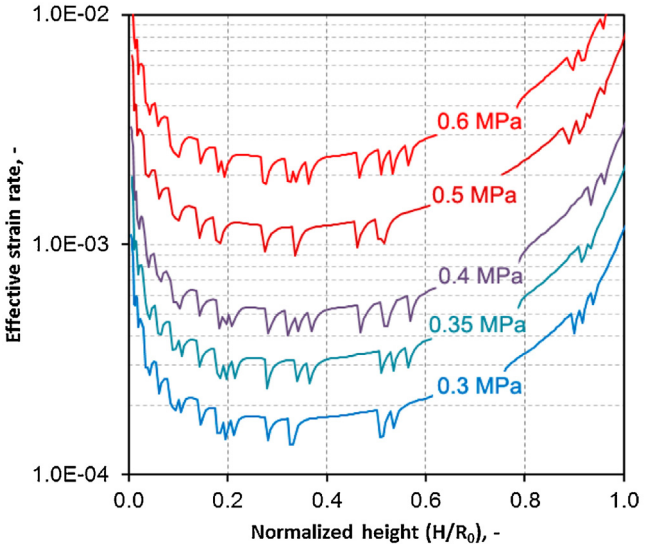

Fig. 6. Effective strain rate vs. normalized dome height relations obtained by simulation of free bulging tests performed at different pressures.

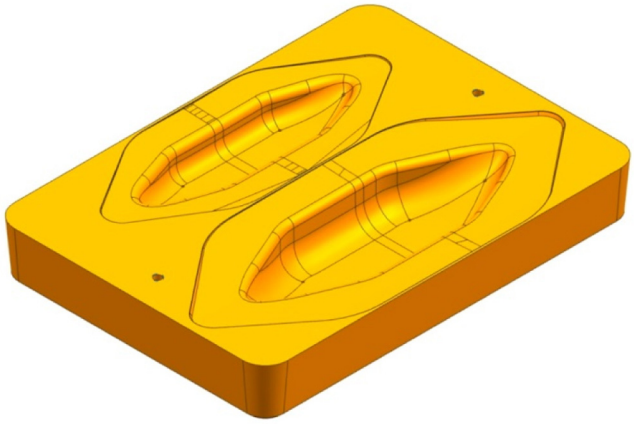

Fig. 7. The geometry of the die.

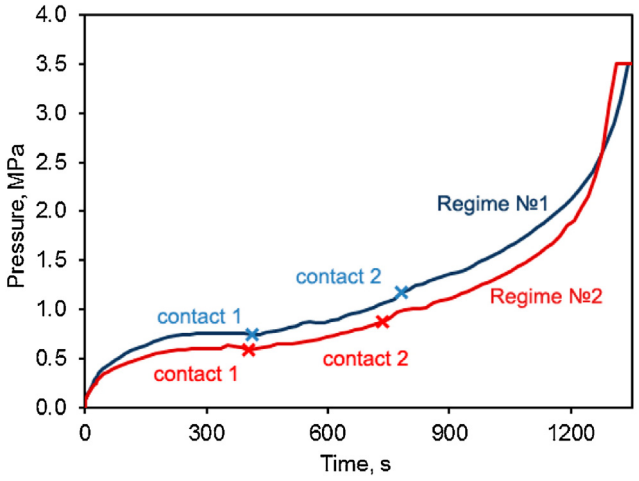

Fig. 8. The pressure regimes obtained using the material constants obtained by free bulging (regime №1) and tensile (regime №2) testing.

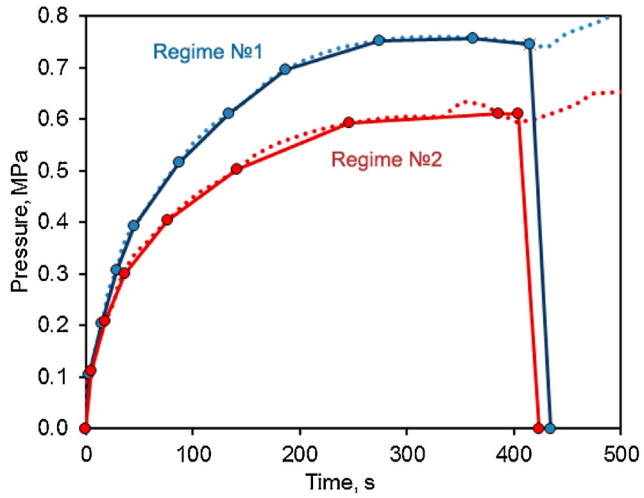

Fig. 9. The smoothened pressure regimes realized in experiments (solid lines) comparing with the initial ones (dotted lines).

dome heights higher when 50 mm correspond to strain values that higher than 0.6 where the power law strain hardening model is incorrect. Using of the constitutive model with nonzero strain hardening results in larger deviations from the experimental data. In further consideration only Backofen constitutive models obtained by different experimental techniques are considered.

In free bulging tests the strain rate at the dome pole is not constant during the forming process. The strain rate evolutions obtained by FEM simulations were produced in order to refine the strain rate values estimated in Section 2.2. The Backofen constitutive model with the constants obtained for biaxial case was used for these simulations. Fig. 6 illustrates how the strain rate depends on normalized dome height (H/R_0) during the tests performed at different constant pressures. It can be seen that the effective strain rate values covers the range of 1.5×10^{-4}–1.0×10^{-2} which is somehow wider than the one estimated in Section 2.2.

3.2. Calculation of pressure regimes for industrial forming

Realization of an SPF or quasi-SPF technology needs the pressure regime controlling the strain rate in the material volume at a predominate level (Chumachenko et al., 2005). Different algorithms of pressure regime calculation could be implemented (Jarrar et al., 2010). The most common and easiest of them is the one maintaining the maximum strain rate value at a constant level.

MSC.MARC was implemented to calculate a pressure regime for a forming of an aircraft part. Rectangular sheet was formed in a die with two cavities of a complex hexagonal shape shown in the Fig. 7. Four-node shell elements were used in the simulation. Two pressure regimes were calculated using the rheological data obtained by the tensile test and by the free bulging test series. The pressure regimes were calculated to maintain the maximum strain rate at the value of $10^{-3}\,s^{-1}$. The results are illustrated in Fig. 8, the moments of contact with the die for each cavity are pointed by the markers.

It can be noticed that the pressure is different in about 20%. The values of pressure obtained by calculations using the tensile tests data are lower than ones obtained using the bulging tests almost at each moment of forming excluding the final one. The moments of contact between the specimen and the die cavities are slightly different: at the first case the contact occurs a bit earlier than at the second one. This can be explained by that the m value obtained by tensile testing (first case) is a slightly larger than the one obtained by the free bulging tests (second case).

This conclusion can be made on the base of the fact that the strain rate sensitivity index m is responsible for flow localization and thus

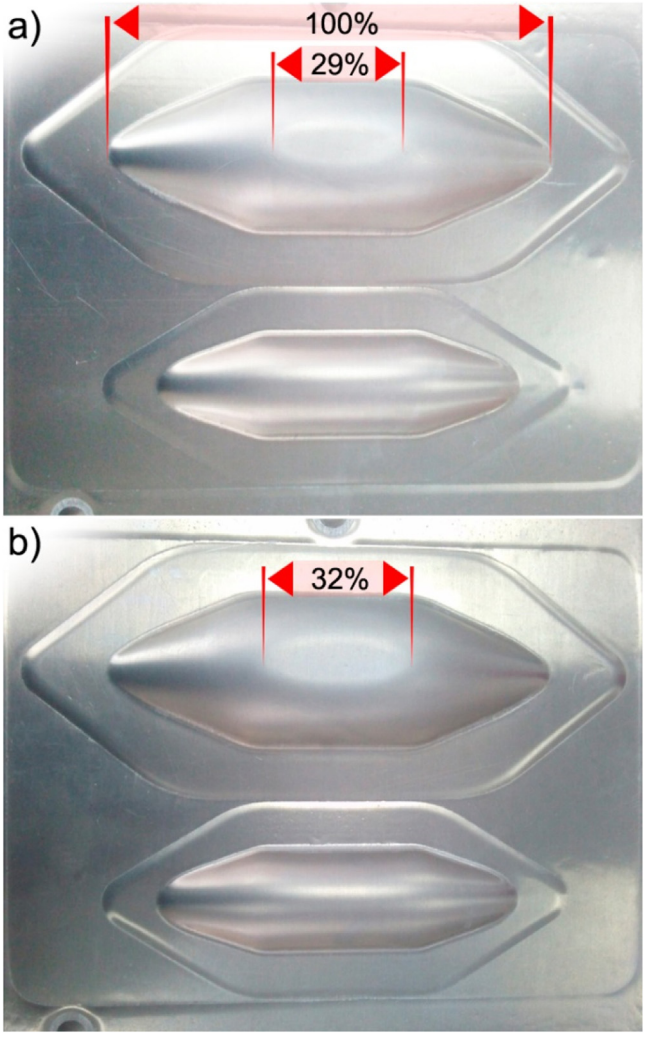

Fig. 10. The specimens after the forming by pressure regime №1.

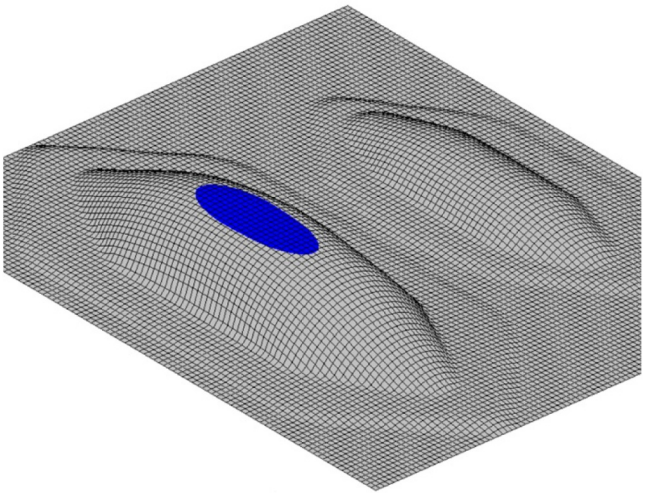

Fig. 11. The results of the FE simulation showing the contact area of the sheet and the die.

Fig. 12. The specimen formed by pressure regime №2.

dictates the difference between minimum and maximum thickness of the specimen. Giuliano and Franchitti (2007) investigated how the material constants affect a specimen thickness at a bulge apex. They show that the specimen thickness corresponding to specific bulge height is affected only by values of m and n and invariant to the value of K. Larger values of m provides lower reduction of thickness at the apex of a bulge. As the pressure regimes were calculated in order to maintain the maximum strain rate which corresponds to a bulge apex the rate of thickness reduction should be the same for booth cases. Thus, higher value of m results in lower reduction and shorter time to contact.

4. Experimental verification, results and discussion

As it was shown above the constitutive equations obtained for a material in uniaxial stress sate and biaxial one can be different which results in that the FEM simulations performed on their base provide different pressure regimes for a particular forming technology. Two cases of pressure regime obtained in previous section were realized in experiments to the moment of first contact and compared with the predictions made by FEM.

As the forming process should be stopped at the incomplete stage, the pressure regimes were reduced to a moment of contact. Moreover in order to meet the accuracy requirements of the equipment, the initial pressure grimes were smoothen and appended with a pressure relief interval as it is shown in Fig. 9.

Forming process was realized on ACB superplastic forming press Loire-SPF 60T equipped with high accuracy gas management system. Argon was used as a working gas. Three shells were formed according to the pressure regimes presented in Fig. 9. Two of them were formed by the regime №1 in order to validate the repeatability of the experiment. The third one was formed using the pressure regime №2. The comparison of the samples formed by the first regime is presented in Fig. 10. It can be noticed, that the formed samples have almost the same shape. Each sample contains to bulges generated by forming to the die cavities. The larger ones have a spot formed by contact with the die surface. The lengths of the contact spots were found to be a 29% and 32% of a part base as it is noted in the Fig. 10. The heights of the smaller bulges were measured at 14.7 mm and 14.8 mm.

Additional finite element simulations were performed using the pressure regimes presented in Fig. 9 to take into account the effect of smoothening and pressure relief interval. The results of the simulation according to the first pressure program and biaxial rheological characteristics are presented in Fig. 11. It can be seen that dew to the prolongation of forming process on about 20 s for the pressure relief the specimen touched the die with forming of a contact spot. The length of the contact spot was found to be a 31% of the part base which is very close to the experimental results. The

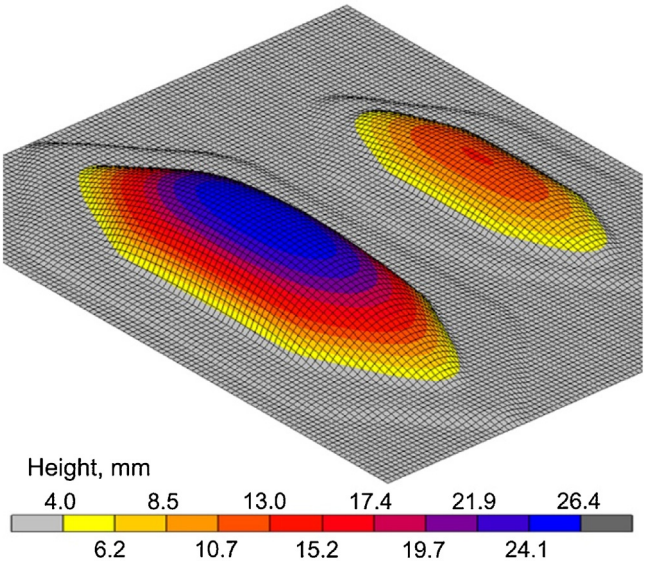

Fig. 13. The results of the FE simulation of the forming performed by pressure regime №2 using the constitutive constants obtained by tensile testing.

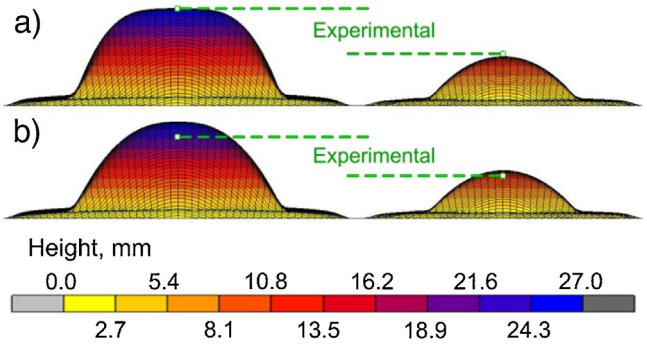

Fig. 14. The comparison between the results of simulations and the measured values of thickness after the forming by the pressure regimes №1 a) and №2 b).

error of the predicted contact spot size is in the range of experimental and measurement deviations. The predicted height of the smaller bulge is 13.7 mm which differs with the experimental value on about 7%.

The thickness of specimen was measured in the points corresponding to the apex of smaller bulge and the center of contact spot of the larger one at 0.90 ± 0.5 and 0.79 ± 0.5 mm. The predicted values for the same points are: 0.919 and 0.869 mm.

The photograph of the sample formed by the pressure regime №2 is presented in Fig. 12. It can be seen, that the specimen did not come in to a contact with the die. The heights of the bulges were measured at 22.7 mm and 11.9 mm. The results of computer simulation of this forming process are presented in Fig. 13. In this simulation the heights of larger and smaller bulges were predicted at 26.9 mm and 13.4 mm. The fact that there is no contact between the specimen and the die in the simulation is explained by the smoothening of forming pressure curve which reduces the pressure values. The results of experiment and predictions made by FEM for the larger bulge differ by 4.2 mm which is more than 18% of the measured height. The deviation between the experiment and the model for the smaller bulge is 1.5 mm or 13% of the measured value. The comparison between the models and experimental results for the both pressure regiems is shown in Fig. 14. The meashured height of both cavities is denoted by green markers and dushed lines.

For the specimen formed by pressure regime №2, the thickness in the apex of the smaller bulge was measured at 0.95 ± 0.05 mm while the predicted value is 0.917 mm. For the larger bulge the measured value of thickness is 0.86 ± 0.05 mm and the predicted one is 0.868 mm. The predicted thickness values are very similar for both regimes. The difference between the experimental and predicted values is comparable with a measurement error.

The results of the experiments and additional simulations show that the forming regime calculated using a constitutive data obtained by tensile tests underestimates the pressure required for the forming process. That results in a fact that during the forming the blank fills the die later than it predicted.

5. Conclusions

The behavior of AMg6 aluminum alloy at 415 °C in conditions of uniaxial and biaxial tension was studied by tensile and free bulging testing. The effective stresses obtained by the results of free bulging tests are higher than the ones obtained by tensile testing both at constant strain rate tests and at the ones with stepped strain rate changing.

Using the constitutive constants obtained by tensile tests in a FEM simulation of free bulging process at constant pressure results in a very fast growth of a predicted dome height. The time needed to form a dome of a particular height according to these predictions is about a half of the one taken from the experimental data.

When the pressure regime is calculated in order to control the strain rate in a specimen at a constant level the pressure values obtained by FE simulation with tensile test constitutive data are lower than the ones corresponded to free bulging tests. Thus the blank during the forming fills the die later than it predicted. At the same time the minimum thickness values at the moment of contact between the specimen and the die are very similar.

Free bulging tests provide the reliable constitutive equations which can be used for accurate simulation of forming processes in a FEM based systems.

Acknowledgements

The study was implemented in the framework of the Basic Research Program at the National Research University Higher School of Economics (HSE).

References

Abu-Farha, F., Khraisheh, M., 2007. Analysis of superplastic deformation of AZ31 magnesium alloy. Adv. Eng. Mater. 9 (9), 777–783.
Aksenov, S.A., Chumachenko, E.N., Kolesnikov, A.V., Osipov, S.A., 2015. Determination of optimal gas forming conditions from free bulging tests at constant pressure. J. Mater. Process. Technol. 217, 158–164.
Aksenov, S.A., Zakhariev, I.Y., Kolesnikov, A.V., Osipov, S.A., 2016. Characterization of superplastic materials by results of free bulging tests. Mater. Sci. Forum 838–839, 552–556.
Alabort, E., Putman, D., Reed, R.C., 2015. Superplasticity in Ti–6Al–4 V: characterisation, modelling and applications. Acta Mater. 95, 428–442.
Albakri, M., Abu-Farha, F., Khraisheh, M., 2013. A new combined experimental–numerical approach to evaluate formability of rate dependent materials. Int. J. Mech. Sci. 66, 55–66.
Backofen, W.A., Turner, I.R., Avery, D.H., 1964. Superplasticity in an Al–Zn alloy. Trans. ASM 57 (4), 980–990.
Chumachenko, E.N., Portnoi, V.K., Paris, L., Billaudeau, T., 2005. Analysis of the SPF of a titanium alloy at lower temperatures. J. Mater. Process. Technol. 170, 448–456.
Chuvil'deev, V.N., Kopylov, V.I., Gryaznov, M.Yu., Sysoev, A.N., Ovsyannikov, B.V., Flyagin, A.A., 2008. Doubling of the strength and plasticity of a commercial aluminum-based alloy (AMg6) processed by equal channel angular pressing. Dokl. Phys. 53 (11), 584–587.
El-Morsy, A., Akkus, N., Manabe, K., Nishimura, H., 2001. Superplastic characteristics of Ti-alloy and Al-alloy sheets by multi-dome forming test. Mater. Trans. 42 (11), 2332–2338.
Enikeev, F.U., Kruglov, A.A., 1995. An analysis of the superplastic forming of a thin circular diaphragm. I. J. Mech. Sci. 37 (5), 473–483.

Giuliano, G., Franchitti, S., 2007. On the evaluation of superplastic characteristics using the finite element method. Int. J. Mach. Tools Manuf. 47, 471–476.
Guo, N.C., Luo, Z.J., Gong, Q.Y., 1990. The superplasticity of commercial aluminium alloy. J. Mater. Process. Technol. 21, 285–294.
Jarrar, F.S., Hector, L.G., Khraisheh, M.K., Bower, A.F., 2010. New approach to gas pressure profile prediction for high temperature AA5083 sheet forming. J. Mater. Process. Technol. 210, 825–834.
Kaibyshev, O.A., 1984. Superplasticity of industrial alloys, Moscow. Metallurgy, 264 (in Russian).
Li, G.Y., Tan, M.J., Liew, K.M., 2004. Three-dimensional modeling and simulation of superplastic forming. J. Mater. Process. Technol. 150, 76–83.
Luckey Jr., G., Friedman, P., Weinmann, K., 2009. Design and experimental validation of a two-stage superplastic forming die. J. Mater. Process. Technol. 209, 2152–2161.
Nazzal, M., Abu-Farha, F., Curtis, R., 2011. Finite element simulations for investigating the effects of specimen geometry in superplastic tensile tests. J. Mater. Eng. Perform. 20, 865–876.
Portnoy, V.K., Rylov, D.S., Levchenko, V.S., Mikhaylovskaya, A.V., 2013. The influence of chromium on the structure and superplasticity of Al–Mg–Mn alloys. J. Alloys Compd. 581, 313–317.
Raman, H., Luckey, S.G., Friedman, P.A., Kridli, G., 2007. Development of accurate constitutive models for simulation of superplastic forming. J. Mater. Eng. Perform. 16 (3), 284–292.
Rusakov, G.M., Illarionov, A.G., Loginov, Yu.N., Lobanov, M.L., Redikul'tsev, A.A., 2015. Interrelation of crystallographic orientations of grains in aluminum alloy AMg6 under hot deformation and recrystallization. Met. Sci. Heat Treat. 56 (11–12), 650–655.
Sorgente, D., Tricarico, L., 2014. Characterization of a superplastic aluminium alloy ALNOVI-U through free inflation tests and inverse analysis. Int. J. Mater. Form. 7, 179–187.
Valiev, R.Z., Kaibyshev, O.A., 1983. On the quantitative evaluation of superplastic flow mechanisms. Acta Metall. 31 (12), 2121–2128.
Woo, S.S., Kim, Y.R., Shin, D.H., Kim, W.J., 1997. Effects of Mg concentration on the quasi-superplasticity of coarse-grained Al-Mg alloys. Scr. Mater. 37 (9, 1), 1351–1358.
Zhao, B., Li, Z., Hou, H., Liao, J., Bai, B., 2010. Three dimensional FEM simulation of titanium hollow blade forming process. Rare Met. Mater. Eng. 39 (6), 963–968.